



Long exciton lifetimes in stacking-fault-free wurtzite GaAs nanowires

Stephan Furthmeier, Florian Dirnberger, Joachim Hubmann, Benedikt Bauer, Tobias Korn, Christian Schüller, Josef Zweck, Elisabeth Reiger, and Dominique Bougeard

Citation: [Applied Physics Letters](#) **105**, 222109 (2014); doi: 10.1063/1.4903482

View online: <http://dx.doi.org/10.1063/1.4903482>

View Table of Contents: <http://scitation.aip.org/content/aip/journal/apl/105/22?ver=pdfcov>

Published by the [AIP Publishing](#)

Articles you may be interested in

[Vapor liquid solid-hydride vapor phase epitaxy \(VLS-HVPE\) growth of ultra-long defect-free GaAs nanowires: Ab initio simulations supporting center nucleation](#)

[J. Chem. Phys.](#) **140**, 194706 (2014); 10.1063/1.4874875

[Self-catalyzed GaAs nanowire growth on Si-treated GaAs\(100\) substrates](#)

[J. Appl. Phys.](#) **109**, 094306 (2011); 10.1063/1.3579449

[Growth of size and density controlled GaAs / In_xGa_{1-x}As / GaAs \(x = 0.10 \) nanowires on anodic alumina membrane-assisted etching of nanopatterned GaAs](#)

[J. Vac. Sci. Technol. B](#) **28**, 1111 (2010); 10.1116/1.3498753

[Observation of free exciton photoluminescence emission from single wurtzite GaAs nanowires](#)

[Appl. Phys. Lett.](#) **94**, 133105 (2009); 10.1063/1.3104853


[Nearly intrinsic exciton lifetimes in single twin-free GaAs/AlGaAs core-shell nanowire heterostructures](#)

[Appl. Phys. Lett.](#) **93**, 053110 (2008); 10.1063/1.2967877

The advertisement features a dark background with a grid pattern. On the left, there is a 3D cutaway illustration of a cylindrical component with a red interior and a blue exterior, showing a light beam passing through it. The text 'Over 600 Multiphysics Simulation Projects' is prominently displayed in white and blue. A blue button with the text 'VIEW NOW >>' is located to the right of the text. The COMSOL logo is in the bottom right corner.

Over **600** Multiphysics Simulation Projects

[VIEW NOW >>](#)

 COMSOL

Long exciton lifetimes in stacking-fault-free wurtzite GaAs nanowires

Stephan Furthmeier,^{a)} Florian Dirnberger, Joachim Hubmann, Benedikt Bauer, Tobias Korn, Christian Schüller, Josef Zweck, Elisabeth Reiger, and Dominique Bougeard
Institut für Experimentelle und Angewandte Physik, Universität Regensburg, D-93040 Regensburg, Germany

(Received 18 September 2014; accepted 23 November 2014; published online 4 December 2014)

We present a combined photoluminescence and transmission electron microscopy study of single GaAs nanowires. Each wire was characterized both in microscopy and spectroscopy, allowing a direct correlation of the optical and the structural properties. By tuning the growth parameters, the nanowire crystal structure is optimized from a highly mixed zincblende–wurtzite structure to pure wurtzite. We find the latter one to be stacking-fault-free over nanowire lengths up to 4.1 μm . We observe the emission of purely wurtzite nanowires to occur only with polarization directions perpendicular to the wurtzite \hat{c} -axis, as expected from the hexagonal unit cell symmetry. The free exciton recombination energy in the wurtzite structure is 1.518 eV at 5 K with a narrow linewidth of 4 meV. Most notably, these pure wurtzite nanowires display long carrier recombination lifetimes of up to 11.2 ns, exceeding reported lifetimes in bulk GaAs and state-of-the-art 2D GaAs/AlGaAs heterostructures. © 2014 AIP Publishing LLC. [<http://dx.doi.org/10.1063/1.4903482>]

Catalytically grown nanowires (NWs) have recently unveiled a unique access to the wurtzite-type (WZ) phase of GaAs^{1–5} which is thermodynamically unstable in bulk or thin film GaAs crystals. This wurtzite phase is stabilized by the large surface-area-to-volume ratio in nanowires and opens new perspectives in the physics of GaAs. Indeed, the reduced symmetry of the hexagonal lattice, compared to the cubic zincblende (ZB), for example, induces spontaneous polarization effects,⁶ but also a different band structure.^{7–9} The resulting optical characteristics and selection rules promise interesting properties for optical spin injection and might also open novel means of band structure engineering within single GaAs NWs through controlled ZB–WZ superlattices.¹⁰ It is currently still challenging to reproducibly grow long NW segments of pure WZ phase^{4,9,11–16} as well as to control the switching of WZ to ZB,^{3,17–19} impeding the experimental exploration of the characteristic properties of pure and stacking-fault (SF)-free WZ GaAs and the validation of theoretical predictions.^{7–9,12–16,20}

In this letter, we investigate single GaAs NWs grown by molecular beam epitaxy (MBE) in successive microphotoluminescence (μ -PL) spectroscopy and transmission electron microscopy (TEM) analyses of each wire. Tuning of the MBE parameters enables the growth of defect-free pure WZ NWs up to 4.1 μm in length, allowing us to study the optical properties of the WZ crystal phase of GaAs. Most strikingly, in time-resolved μ -PL, the pure WZ structure is characterized by particularly long carrier lifetimes compared to pure ZB and polytypic ZB/WZ GaAs NWs,^{17,22,23} pointing towards an inherently reduced oscillator strength of the ground state optical transition in WZ GaAs NWs.

The GaAs NWs were synthesized by MBE using the Au-assisted vapor–liquid–solid growth mechanism^{24,25} on GaAs(111)_B substrates covered with 10 Å Au. After transferring the substrates into the MBE growth chamber, the native oxide was initially removed at temperatures above 600 °C, followed by the actual NW growth at a lower temperature

of 510 °C. The NWs were passivated with a uniform Al_{0.3}Ga_{0.7}As shell with a thickness of \sim 10 nm in order to disable the dominant nonradiative recombination at the bare GaAs surface.^{23,26} This shell was surrounded by a \sim 5 nm GaAs cap to protect the Al_{0.3}Ga_{0.7}As layer from oxidation.²⁷

For the correlated optical and structural characterization of a single wire, the NWs were removed from the substrate by ultrasonication and dispersed on 5 nm thick amorphous Si TEM membranes. As the electron beam exposure in the TEM has been proven to deteriorate the optical properties of NWs,²⁸ all PL measurements were carried out prior to the TEM survey. We first performed spatially resolved μ -PL measurements in order to preselect NWs with different crystalline purities. The NWs of interest were then individually further investigated by polarization- and time-resolved μ -PL before fully characterizing their crystal structure with TEM. The PL measurements were conducted in a confocal configuration at 5 K using both continuous-wave (cw) and pulsed excitation. Single NWs were excited with the 690 nm emission line (\sim 1.8 eV) of a semiconductor laser diode operating in cw or pulsed mode (70 ps pulses at a repetition rate of 1 MHz). A 100 \times microscope objective with NA = 0.8 focused the laser light down to the sample with a spot diameter of around 1 μm . The emitted PL was collected by the same objective and imaged onto the entrance slit of a grating spectrometer. Spatially and polarization-resolved μ -PL spectra were acquired using a liquid nitrogen cooled charge coupled device, while time-resolved PL (TRPL) signals were detected by a Hamamatsu streak camera system. In both setups, piezoelectric x-y-z translation stages enable fine mapping of the emitted PL. For the polarization-dependent measurements, a linear polarizer followed by a half-wave plate allowed a continuously adjustable polarization of the exciting laser light from parallel to perpendicular to the NW axis, while an additional linear polarizer was used for analyzing the linear PL polarization properties. The structural characterization was performed in a FEI Tecnai F30 TEM operated at 300 kV using high resolution TEM (HRTEM) imaging and electron diffraction.

^{a)}Electronic mail: stephan.furthmeier@ur.de

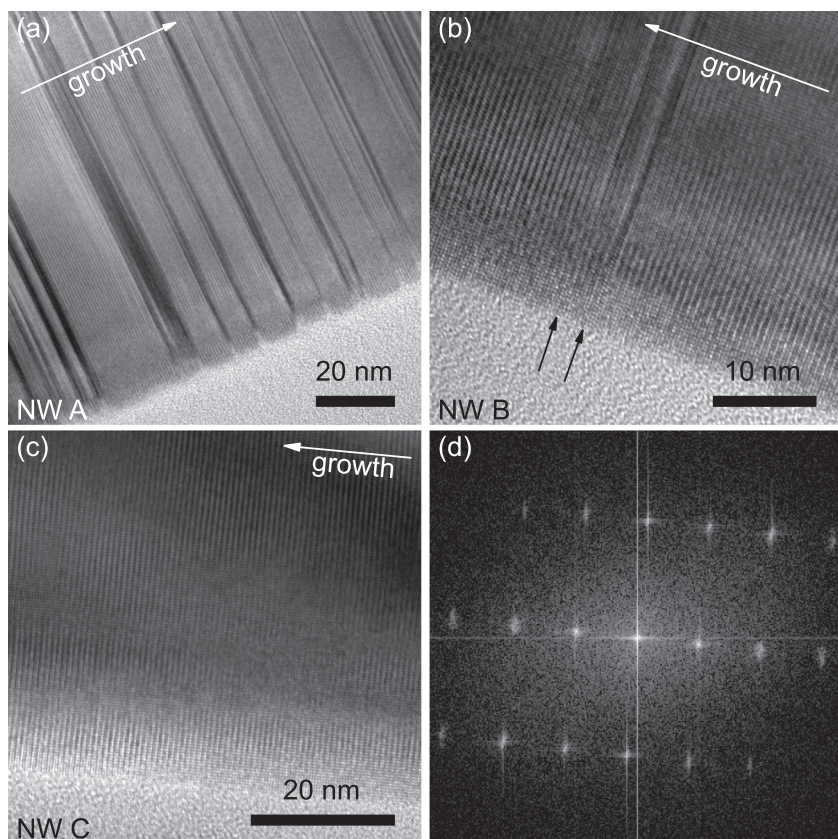


FIG. 1. (a)–(c) Representative high-resolution TEM micrographs of the three GaAs NWs A, B, and C presented in this letter, respectively. The black arrows in (b) mark two single SFs identified in wire B. (d) Fast Fourier transform of the HRTEM image in (c) taken from the SF-free NW C and showing the typical spot pattern of a pure WZ structure.

We optimized the crystalline structure of our GaAs NWs through tuning of MBE growth parameters. In this study, the Ga deposition rate, calibrated via RHEED-oscillations, was kept constant at 0.4 \AA/s , while the As_4 -flux was adjusted. Lowering the As_4 beam equivalent pressure from $3.0 \times 10^{-6} \text{ Torr}$ to $1.5 \times 10^{-6} \text{ Torr}$ allowed us to tune the crystalline structure of the NWs from polytypic WZ/ZB to SF-free, pure WZ over lengths of several μm . We exemplarily discuss three single wires labeled A, B, and C, which are characteristic for the obtained tunability range. Figure 1 shows representative HRTEM micrographs of the three wires, each of which was comprehensively analyzed with HRTEM over the entire length. As revealed by Fig. 1(a), wire A—highest As_4 -flux—is composed of a strongly mixed WZ–ZB structure, characterized by a spatially inhomogeneous distribution of multiple SFs. A careful evaluation of the HRTEM images along the entire wire reveals an overall SF density of approximately $100 \text{ SF}/\mu\text{m}$. A significantly improved crystal structure is observed for wires B and C grown under lower As_4 -fluxes. Wire B already comprises a dominant WZ GaAs phase without any ZB inserts, but still some SFs, as illustrated in Fig. 1(b). By analyzing the complete NW in HRTEM, we identified a total of 8 SFs, well separated from each other with the smallest distance between two SFs being 3 nm. Wire C—lowest As_4 -flux—consists of a pure, defect-free WZ GaAs crystal phase with not even one SF along its entire length of $4.1 \mu\text{m}$, as verified in HRTEM. The presence of a pure WZ structure is also confirmed by the corresponding pattern in reciprocal space obtained by fast Fourier transform and shown in Fig. 1(d).

Before the TEM analysis, we have analyzed each of the three wires in spatially resolved μ -PL, allowing us to connect

the emission spectra of the NWs with their respective crystalline structure. Spatially resolved spectra of the wires A and C, obtained with low power ($\sim 5 \text{ W/cm}^2$) cw excitation, are shown in Fig. 2. It can be seen from Fig. 2(a) that the PL emission of the defect-rich wire A ($\sim 100 \text{ SF}/\mu\text{m}$) comprises typical SF-related PL features characterized by several peaks with different energies and linewidths, originating from the different parts of the NW. Indeed, the coupling between

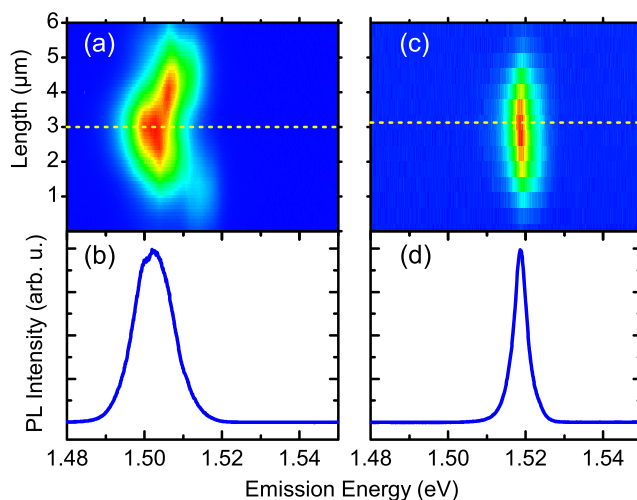


FIG. 2. (a) False-color low temperature (5 K) μ -PL spectra as a function of position along the defect-rich WZ GaAs NW A with the high SF density of $\sim 100 \text{ SF}/\mu\text{m}$. The PL emission extends along its entire length of $6.0 \mu\text{m}$. (b) Typical μ -PL spectrum recorded at the position of the dashed line in (a). (c) Spatially resolved μ -PL at 5 K from the SF-free WZ GaAs NW C. The wire emits along its entire length of $4.1 \mu\text{m}$. (d) μ -PL spectrum recorded at the position of the dashed line in (c).

adjacent SFs can cause the formation of minibands with additional electronic states and thus modify the PL emission, as has already been detected in rotationally twinned InP NWs²⁹ and polytypic ZB/WZ GaAs NWs.^{12,17–19} Consequently, all the emission lines in Fig. 2(a) have energies smaller than the free exciton recombination in ZB GaAs ($E = 1.515$ eV).³⁰ A μ -PL spectrum recorded at the position marked with the dashed line is depicted in Fig. 2(b). The total PL is rather broad with a full width at half maximum (FWHM) of about 13 meV centered around 1.501 eV. In contrast, the PL emission from the SF-free wire C is characterized by only a single emission peak at 1.518 eV, as illustrated in Fig. 2(c). In particular, this peak is present over the entire length of the wire and shows no significant shift along the way, neither in energy nor in spectral linewidth and almost independently of excitation power. Hence, as no defect-related luminescence is observed, the spatially resolved μ -PL analysis demonstrates that this pure WZ GaAs NW is of very high crystalline and optical quality. The spatially resolved μ -PL of wire B with 8 SFs (not shown) looks similar to Fig. 2(c), which suggests that the existence of a few separated SFs does not strongly affect the optical properties. A typical PL spectrum of the defect-free WZ GaAs NW C is presented in Fig. 2(d). The emission is determined by a single peak centered at 1.518 eV, confirming some theoretical studies⁷ and experimental observations in similar, but not purely WZ NWs.^{9,13,15,16,20} Notably, the FWHM of 4 meV observed here is one of the narrowest reported in single GaAs NWs until now. Since the crystalline purity is verified with TEM, we attribute this peak to the free exciton recombination in WZ GaAs with an emission energy of 1.518 eV, 3 meV larger than in the ZB phase.

The WZ character of wire C is further confirmed by the polarization characteristics of its PL emission. Indeed, due to the lower symmetry of the hexagonal WZ unit cell compared to ZB, only transitions inducing emission polarized perpendicular to the \hat{c} -axis are expected to be allowed in pure WZ NWs.²¹ The linear polarization-dependence of the PL emission relative to the NW axis for the defect-free wire C is shown in Fig. 3(a) as a false-color plot. While the emission energy is constant as depicted in Fig. 2(d), the PL intensity varies π -periodically as a function of the polarization analyzer angle. Figure 3(b) displays the extracted azimuthal dependence of the integrated PL intensity for this wire. The polarization of the excitation laser was always chosen parallel to the NW growth direction, ensuring that the recorded linearly polarized PL emission reflects the intrinsic properties of the investigated WZ excitonic ground state. Strong maxima are observed for emission polarized perpendicular to the NW axis which, according to TEM, corresponds to the \hat{c} -axis of the WZ unit cell, underlining the high WZ purity of wire C. As can be noted in Fig. 3(b), the integrated PL intensity does not completely vanish at zero polarization angle despite the optical selection rules. We determine a degree of linear polarization of 71% with a $\cos^2\theta$ least-squares fit to the data. This deviation from 100% is a result of the well-known refractive index mismatch effect, which favors parallel emission due to the high dielectric contrast between the NW and its environment (vacuum).²¹ It has also been observed in ZB GaAs NWs, where the intrinsically unpolarized free exciton emission is found to be highly polarized along the wire axis.^{31,32}

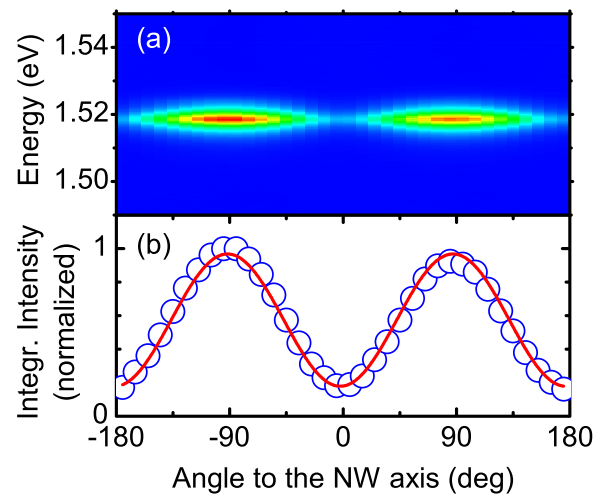


FIG. 3. Polarization-resolved μ -PL from the defect-free WZ GaAs NW C. (a) False-color plot of PL emission spectra as a function of the angle to the NW axis. The polarization of the excitation is always aligned along the NW. (b) Integrated PL intensity as a function of the angle to the NW axis. The continuous red line is a $\cos^2\theta$ fit to the data obtained with the Jones matrix formalism. The PL polarization direction is determined from this fit to be at 89.1° to the NW axis with a degree of linear polarization of 71%.

In order to evaluate the impact of the hexagonal WZ crystal structure on the dynamics of the free exciton recombination, NW C was further characterized by time-resolved PL. Figure 4(a) displays the time evolution of the μ -PL signal photoexcited by 70 ps pulses at 690 nm with a time-averaged power of 10 W/cm². The time decay is extracted from the streak data collected at the energy of the free exciton emission and shown in Fig. 4(b). We observe neither a significant blue shift of the PL emission compared to the emission induced by cw excitation nor an increase of the FWHM, excluding state filling effects, despite of much higher peak powers of approximately 140 kW/cm² under pulsed operation compared to the previous cw experiments.

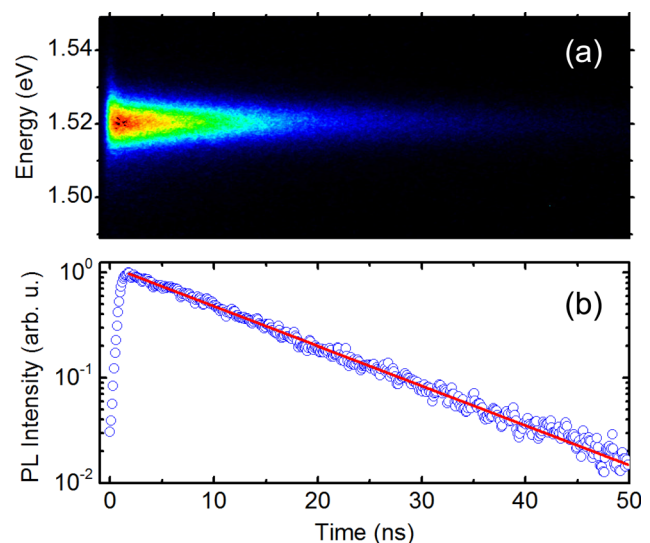


FIG. 4. (a) Time-resolved streak image of the defect-free WZ GaAs NW C measured at 5 K. (b) Time decay of the PL peak from (a). The transient is fitted with a single exponential (continuous red line) consistent with a pure excitonic emission. The spectral range considered is ~ 6 meV wide, centered around the narrow PL peak, and the extracted free exciton recombination lifetime is 11.2 ns.

We can also exclude the formation of an electron–hole plasma, which would induce a fast decay at the initial stages of the relaxation process, since the decay observed in Fig. 4(b) is monoexponential.^{22,33} This monoexponential decay thus reflects the pure excitonic emission in the GaAs WZ structure. The extracted exciton lifetime of 11.2 ns clearly exceeds the reported values of WZ GaAs NWs,^{15,16} ZB GaAs NWs,^{22,23} and high-quality ZB/WZ GaAs NW heterostructures.¹⁷ The measured decay time is also longer than intrinsic exciton recombination lifetimes in pure ZB structures like bulk GaAs and 2D GaAs/AlGaAs wide double heterostructures.³⁰ Note that our experiment gives the lower limit, as the observed PL lifetime can be expected to be shortened by non-radiative recombination channels at the GaAs/AlGaAs core–shell interface.^{23,34} In general, long excitonic lifetimes in NWs have been attributed to local charge separation induced by crystal phase mixing.^{17,35} As we can exclude this mechanism for the SF-free wire C, the observed long PL lifetime seems to be directly related to the WZ crystal phase and thus points towards a lower oscillator strength of the ground state optical transition in WZ GaAs NWs compared to ZB GaAs NWs.

In conclusion, we have demonstrated MBE of pure WZ GaAs in NWs featuring SF-free lengths of up to 4.1 μm . The purely WZ crystal structure is confirmed by HRTEM imaging and the polarization characteristics of the PL emission. The free exciton emission energy in the WZ phase of GaAs is found to be 1.518 eV, 3 meV larger than its ZB counterpart. Strikingly, with 11.2 ns, the carrier recombination lifetime of the excitonic transition in WZ GaAs NWs exceeds all values reported so far for (polytypic) ZB/WZ GaAs NWs, bulk GaAs, or 2D GaAs/AlGaAs heterostructures. Our study indicates that this long exciton lifetime is an inherent property of high-quality WZ GaAs NWs.

We gratefully acknowledge financial support by the German Research Foundation (DFG) via Grant Nos. SFB 689 and SPP 1285.

¹M. Koguchi, H. Kakibayashi, M. Yazawa, K. Hiruma, and T. Katsuyama, *Jpn. J. Appl. Phys., Part 1* **31**, 2061 (1992).

²F. Glas, J.-C. Harmand, and G. Patriarche, *Phys. Rev. Lett.* **99**, 146101 (2007).

³M. C. Plante and R. R. LaPierre, *Nanotechnology* **19**, 495603 (2008).

⁴H. L. Zhou, T. B. Hoang, D. L. Dheeraj, A. T. J. van Helvoort, L. Liu, J. C. Harmand, B. O. Fimland, and H. Weman, *Nanotechnology* **20**, 415701 (2009).

⁵K. A. Dick, P. Caroff, J. Bolinsson, M. E. Messing, J. Johansson, K. Deppert, L. R. Wallenberg, and L. Samuelson, *Semicond. Sci. Technol.* **25**, 024009 (2010).

⁶B. Bauer, J. Hubmann, M. Lohr, E. Reiger, D. Bougeard, and J. Zweck, *Appl. Phys. Lett.* **104**, 211902 (2014).

⁷A. De and C. E. Pryor, *Phys. Rev. B* **81**, 155210 (2010).

⁸M. Murayama and T. Nakayama, *Phys. Rev. B* **49**, 4710 (1994).

⁹B. Ketterer, M. Heiss, E. Uccelli, J. Arbiol, and A. Fontcuberta i Morral, *ACS Nano* **5**, 7585 (2011).

¹⁰P. Caroff, K. A. Dick, J. Johansson, M. E. Messing, K. Deppert, and L. Samuelson, *Nat. Nanotechnol.* **4**, 50 (2009).

¹¹H. J. Joyce, J. Wong-Leung, Q. Gao, H. H. Tan, and C. Jagadish, *Nano Lett.* **10**, 908 (2010).

¹²M. Heiss, S. Conesa-Boj, J. Ren, H.-H. Tseng, A. Gali, A. Rudolph, E. Uccelli, F. Peiró, J. R. Morante, D. Schuh, E. Reiger, E. Kaxiras, J. Arbiol, and A. Fontcuberta i Morral, *Phys. Rev. B* **83**, 045303 (2011).

¹³B. Ketterer, M. Heiss, M. J. Livrozet, A. Rudolph, E. Reiger, and A. Fontcuberta i Morral, *Phys. Rev. B* **83**, 125307 (2011).

¹⁴P. Kusch, S. Breuer, M. Ramsteiner, L. Geelhaar, H. Riechert, and S. Reich, *Phys. Rev. B* **86**, 075317 (2012).

¹⁵L. Ahtapodov, J. Todorovic, P. Olk, T. Mjåland, P. Slåttnes, D. L. Dheeraj, A. T. J. van Helvoort, B.-O. Fimland, and H. Weman, *Nano Lett.* **12**, 6090 (2012).

¹⁶Z. Lu, S. Shi, J. Lu, and P. Chen, *J. Lumin.* **152**, 258 (2014).

¹⁷D. Spirkoska, J. Arbiol, A. Gustafsson, S. Conesa-Boj, F. Glas, I. Zardo, M. Heigoldt, M. H. Gass, A. L. Bleloch, S. Estrade, M. Kaniber, J. Rossler, F. Peiro, J. R. Morante, G. Abstreiter, L. Samuelson, and A. Fontcuberta i Morral, *Phys. Rev. B* **80**, 245325 (2009).

¹⁸A. M. Graham, P. Corfdir, M. Heiss, S. Conesa-Boj, E. Uccelli, A. Fontcuberta i Morral, and R. T. Phillips, *Phys. Rev. B* **87**, 125304 (2013).

¹⁹P. Corfdir, B. Van Hattem, E. Uccelli, A. Fontcuberta i Morral, and R. T. Phillips, *Appl. Phys. Lett.* **103**, 133109 (2013).

²⁰S. Breuer, C. Pfüller, T. Flissikowski, O. Brandt, H. T. Grahm, L. Geelhaar, and H. Riechert, *Nano Lett.* **11**, 1276 (2011).

²¹C. Wilhelm, A. Larrue, X. Dai, D. Migas, and C. Soci, *Nanoscale* **4**, 1446 (2012).

²²L. M. Smith, H. E. Jackson, J. M. Yarrison-Rice, and C. Jagadish, *Semicond. Sci. Technol.* **25**, 024010 (2010).

²³O. Demichel, M. Heiss, J. Bleuse, H. Mariette, and A. Fontcuberta i Morral, *Appl. Phys. Lett.* **97**, 201907 (2010).

²⁴R. S. Wagner and W. C. Ellis, *Appl. Phys. Lett.* **4**, 89 (1964).

²⁵M. E. Messing, K. Hillerich, J. Johansson, K. Deppert, and K. A. Dick, *Gold Bull.* **42**, 172 (2009).

²⁶C.-C. Chang, C.-Y. Chi, M. Yao, N. Huang, C.-C. Chen, J. Theiss, A. W. Bushmaker, S. LaLumondiere, T.-W. Yeh, M. L. Povinelli, C. Zhou, P. D. Dapkus, and S. B. Cronin, *Nano Lett.* **12**, 4484 (2012).

²⁷S. Perera, M. A. Fickenscher, H. E. Jackson, L. M. Smith, J. M. Yarrison-Rice, H. J. Joyce, Q. Gao, H. H. Tan, C. Jagadish, X. Zhang, and J. Zou, *Appl. Phys. Lett.* **93**, 053110 (2008).

²⁸J. Todorovic, A. F. Moses, T. Karlberg, P. Olk, D. L. Dheeraj, B. O. Fimland, H. Weman, and A. T. J. van Helvoort, *Nanotechnology* **22**, 325707 (2011).

²⁹J. Bao, D. C. Bell, F. Capasso, J. B. Wagner, T. Mårtensson, J. Trägårdh, and L. Samuelson, *Nano Lett.* **8**, 836 (2008).

³⁰G. Gilliland, *Mater. Sci. Eng., R* **18**, 99 (1997).

³¹D. Spirkoska, A. L. Efros, W. R. L. Lambrecht, T. Cheiwchanchamnangij, A. Fontcuberta i Morral, and G. Abstreiter, *Phys. Rev. B* **85**, 045309 (2012).

³²P. Plochocka, A. A. Mitioglu, D. K. Maude, G. L. J. A. Rikken, A. Granados del Águila, P. C. M. Christianen, P. Kacman, and H. Shtrikman, *Nano Lett.* **13**, 2442 (2013).

³³L. V. Titova, T. B. Hoang, J. M. Yarrison-Rice, H. E. Jackson, Y. Kim, H. J. Joyce, Q. Gao, H. H. Tan, C. Jagadish, X. Zhang, J. Zou, and L. M. Smith, *Nano Lett.* **7**, 3383 (2007).

³⁴N. Jiang, Q. Gao, P. Parkinson, J. Wong-Leung, S. Mokkapati, S. Breuer, H. H. Tan, C. L. Zheng, J. Etheridge, and C. Jagadish, *Nano Lett.* **13**, 5135 (2013).

³⁵K. Pemasiri, M. Montazeri, R. Gass, L. M. Smith, H. E. Jackson, J. Yarrison-Rice, S. Paiman, Q. Gao, H. H. Tan, C. Jagadish, X. Zhang, and J. Zou, *Nano Lett.* **9**, 648 (2009).